

## Excitation of vibrational quanta in furfural by intermediate-energy electrons

D. B. Jones, R. F. C. Neves, M. C. A. Lopes, R. F. da Costa, M. T. do N. Varella, M. H. F. Bettega, M. A. P. Lima, G. García, F. Blanco, and M. J. Brunger

Citation: *The Journal of Chemical Physics* **143**, 224304 (2015); doi: 10.1063/1.4936631

View online: <http://dx.doi.org/10.1063/1.4936631>

View Table of Contents: <http://scitation.aip.org/content/aip/journal/jcp/143/22?ver=pdfcov>

Published by the [AIP Publishing](#)

---

### Articles you may be interested in

[Intermediate energy cross sections for electron-impact vibrational-excitation of pyrimidine](#)

*J. Chem. Phys.* **143**, 094304 (2015); 10.1063/1.4929907

[Intermediate energy electron impact excitation of composite vibrational modes in phenol](#)

*J. Chem. Phys.* **142**, 194302 (2015); 10.1063/1.4921038

[Differential cross sections for electron-impact vibrational-excitation of tetrahydrofuran at intermediate impact energies](#)

*J. Chem. Phys.* **142**, 124306 (2015); 10.1063/1.4915888

[Absolute cross sections for vibrational excitations of cytosine by low energy electron impact](#)

*J. Chem. Phys.* **137**, 115103 (2012); 10.1063/1.4752655

[Vibrational excitation of methane by 15 and 30 eV intermediate-energy electron impact](#)

*J. Chem. Phys.* **106**, 5990 (1997); 10.1063/1.473263

---

**Ready, set, simulate.**

**REGISTER FOR THE COMSOL CONFERENCE >>**



## Excitation of vibrational quanta in furfural by intermediate-energy electrons

D. B. Jones,<sup>1</sup> R. F. C. Neves,<sup>1,2,3</sup> M. C. A. Lopes,<sup>3</sup> R. F. da Costa,<sup>4,5</sup> M. T. do N. Varella,<sup>6</sup> M. H. F. Bettega,<sup>7</sup> M. A. P. Lima,<sup>4</sup> G. García,<sup>8</sup> F. Blanco,<sup>9</sup> and M. J. Brunger<sup>1,10,a)</sup>

<sup>1</sup>*School of Chemical and Physical Sciences, Flinders University, GPO Box 2100, Adelaide, South Australia 5001, Australia*

<sup>2</sup>*Instituto Federal do Sul de Minas Gerais, Campus Poços de Caldas, Minas Gerais, Brazil*

<sup>3</sup>*Departamento de Física, Universidade Federal de Juiz de Fora, 36036-900, Juiz de Fora, MG, Brazil*

<sup>4</sup>*Instituto de Física “Gleb Wataghin,” Universidade Estadual de Campinas, Campinas, 13083-859 São Paulo, Brazil*

<sup>5</sup>*Centro de Ciências Naturais e Humanas, Universidade Federal do ABC, Santo André, 09210-580 São Paulo, Brazil*

<sup>6</sup>*Instituto de Física, Universidade de São Paulo, CP 66318, 05315-970 São Paulo, São Paulo, Brazil*

<sup>7</sup>*Departamento de Física, Universidade Federal do Paraná, CP 19044, 81531-990 Curitiba, Paraná, Brazil*

<sup>8</sup>*Instituto de Física Fundamental, CSIC, Serrano 113-bis, 28006 Madrid, Spain*

<sup>9</sup>*Departamento de Física Atómica, Molecular y Nuclear, Universidad Complutense de Madrid, Madrid E-28040, Spain*

<sup>10</sup>*Institute of Mathematical Sciences, University of Malaya, 50603 Kuala Lumpur, Malaysia*

(Received 6 October 2015; accepted 16 November 2015; published online 8 December 2015)

We report cross sections for electron-impact excitation of vibrational quanta in furfural, at intermediate incident electron energies (20, 30, and 40 eV). The present differential cross sections are measured over the scattered electron angular range 10°–90°, with corresponding integral cross sections subsequently being determined. Furfural is a viable plant-derived alternative to petrochemicals, being produced via low-temperature plasma treatment of biomass. Current yields, however, need to be significantly improved, possibly through modelling, with the present cross sections being an important component of such simulations. To the best of our knowledge, there are no other cross sections for vibrational excitation of furfural available in the literature, so the present data are valuable for this important molecule. © 2015 AIP Publishing LLC. [<http://dx.doi.org/10.1063/1.4936631>]

### I. INTRODUCTION

Over the last few years, we have been interested in measuring intermediate-energy electron-impact cross sections, often for bands of composite vibrational quanta, in biomolecules such as water (H<sub>2</sub>O),<sup>1,2</sup> tetrahydrofuran (THF),<sup>3–6</sup>  $\alpha$ -tetrahydrofurfuryl alcohol (THFA),<sup>7</sup> and pyrimidine (Py),<sup>8</sup> and for important products from the application of low-temperature plasmas<sup>9,10</sup> on biomass such as phenol<sup>11,12</sup> and furfural (this paper). There are several reasons for this, with one being to contribute to the creation of “complete” cross section data bases for those species. This is important as, for example, the transport of electrons in those molecules under the influence of an applied electric field might be investigated using a Boltzmann equation analysis,<sup>1,2,4,6</sup> or Monte Carlo techniques might be applied to study the behaviour of charged particles as they traverse gaseous or liquid forms of those species.<sup>13–17</sup> In the former case, the compiled cross section data base can be benchmarked against independently measured transport coefficients (e.g., Ref. 2), while in the latter case the results can be employed to better understand particle range and dose and radiation damage at the nanoscale (e.g., Refs. 16 and 17) as well as the effect of plasma action in biomass.<sup>18,19</sup>

Another reason for studying these species, all of which to one extent or another have some molecular geometry similarities, is to try and better understand the dynamics by which their nuclear degrees of freedom are excited by the incident electron. For instance for some of the composite vibrational modes,<sup>5,7,11</sup> for incident electron energies between 15 and 50 eV, the angular distributions of the cross sections are quasi-isotropic, whereas at those same energies, the elastic angular distributions and the angular distributions for the optically allowed discrete-inelastic electronic states are often strongly peaked in magnitude<sup>20–29</sup> at the smaller scattered electron angles. That latter behaviour is understood in terms of the strong dipole polarisabilities and permanent dipole moments of the molecules in question. We are thus very interested to see if this same quasi-isotropic behaviour in the composite vibrational mode angular distributions is also found with electron scattering from furfural.

Furfural (C<sub>5</sub>H<sub>4</sub>O<sub>2</sub>) is an important chemical in many existing industries,<sup>30</sup> and it has also been suggested as a possible platform chemical<sup>31,32</sup> in the commercial realisation of bio-refineries.<sup>33</sup> Two approaches, atmospheric plasma pre-treatment<sup>18,19</sup> or electron-beam irradiation,<sup>34,35</sup> have been put forward to overcome the natural recalcitrance of biomass and thereby improve furfural yields from, e.g., hemicellulose. A thorough understanding of the quantum structure of furfural, and its electron-driven reaction dynamics, is thus essential in developing innovative approaches that can contribute to

a) Author to whom correspondence should be addressed. Electronic mail: Michael.Brunger@flinders.edu.au

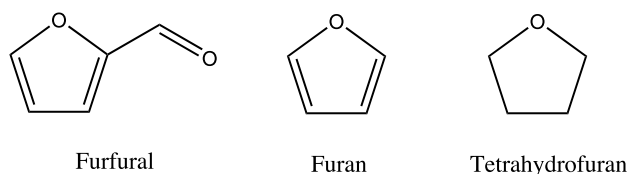


FIG. 1. Schematic diagrams for the structures of the *trans*-conformer of furfural, furan, and tetrahydrofuran.

improving the conversion efficiency of biomass and for the economic realisation of next generation biofuels. This forms a further rationale for the present investigation.

We believe the present study is the first to probe excitation of vibrational quanta in furfural by electron scattering, although some work on its molecular structure and spectroscopy<sup>36</sup> and ionisation dynamics<sup>37</sup> has been published by our team. Nonetheless, we know of no other experimental or theoretical cross sections, either differential or integral, against which we might compare the current results. We have instead chosen to compare our present furfural composite vibrational cross sections to corresponding results from tetrahydrofuran<sup>5</sup> and furan.<sup>38</sup> This comparison enables us to further our broader goals of understanding the role of molecular structure in electron scattering interactions. Here furfural, furan, and THF (see Fig. 1) all possess 5-member rings as their core structures. Both furan and furfural have a common aromatic ring, with furfural only differing by the addition of an exocyclic group. This is different from THF, where the 5-member ring is hydrogenated. We believe that this comparison might be instructive in establishing how common features of molecules may provide some indication of the anticipated electron scattering phenomenon. This has previously proved quite successful through the implementation of calculations at the independent atom model (IAM) with screening corrected additivity rule (SCAR).<sup>39–41</sup> We return to this point in detail later in our Sec. III of the paper.

The remainder of this submission is structured as follows. In Sec. II, we briefly describe our experimental techniques and

the analysis procedures that we employed here. Thereafter, in Sec. III, our results and a discussion of those results are presented. Finally, in Sec. IV, some conclusions from the current investigation are drawn.

## II. EXPERIMENTAL DETAILS

An example of a typical energy loss spectrum (EELS), measured as a part of this investigation, is given in Fig. 2. Those data were taken with a crossed-beam apparatus housed at Flinders University,<sup>42</sup> which has been documented in detail before. Briefly, however, a monochromated beam of electrons with energies ( $E_0$ ) of 20 eV, 30 eV, or 40 eV and a typical flux of 1–6 nA was incident on an orthogonal beam of furfural. Furfural (Sigma Aldrich; 99% assay) was not an easy target to work with, with details of our procedures for obtaining a stable beam now being given. The furfural vapour from a liquid reservoir, heated to  $\sim 40^\circ\text{C}$ , passes through a gas handling system heated to  $60^\circ\text{C}$ , where it is introduced into the heated vacuum chamber ( $T \sim 60^\circ\text{C}$ ) through a variable leak valve which is in turn coupled to a single channel capillary needle (molybdenum) of 0.7 mm inner diameter that acts as the furfural beam-forming device. Note that the sample reservoir, gas handling lines, leak valve, and the scattering chamber were all insulated from their surrounds in order to keep their temperature as stable as possible. Under the stable beam conditions maintained during the EELS measurements, the furfural pressure in the vacuum chamber never exceeded  $2 \times 10^{-5}$  Torr in order to minimise any possible multiple scattering effects. The intersection of the electron and furfural beams defines a collision volume (interaction region), and those electrons which collided with the molecules and scattered at some angle  $\theta$ , called the electron scattering angle, were energy analysed using a hemispherical selector before being detected with a channel electron multiplier. Note that the angular range of the present EELS was  $10^\circ$ – $90^\circ$ , while the angular resolution of the analyser is  $2^\circ$ . Further note that the overall instrumental energy resolution employed

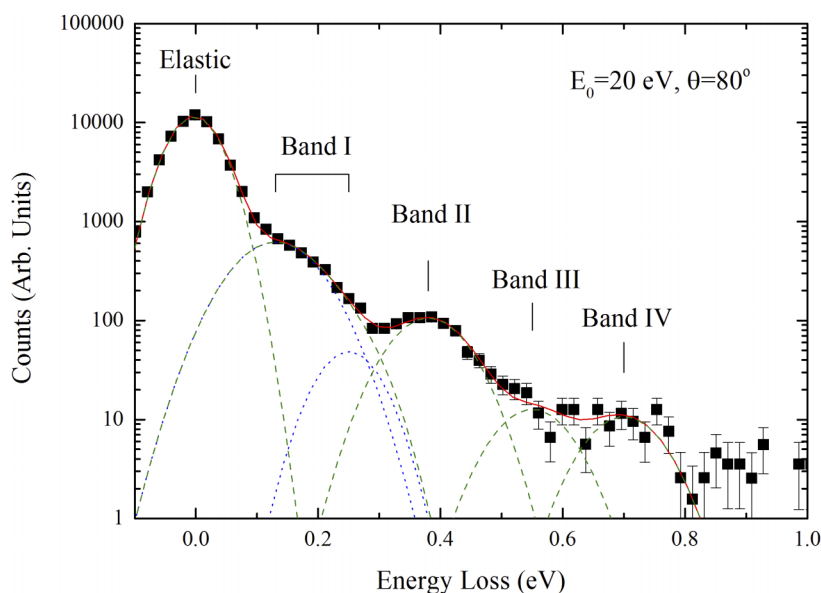


FIG. 2. A typical energy loss spectrum for electron-impact excitation of the composite vibrational modes of furfural (see also Table I). The incident electron energy is 20 eV and the scattered electron angle is  $80^\circ$ , while the energy loss range of interest is  $-0.2$  to 1 eV. The overall spectral deconvolution plot is denoted by the solid red line, while the fits to the various composite vibrational features (bands I–IV) and the elastic peak are also shown by the dotted-blue and dashed-green lines.

TABLE I. The furfural composite vibrational feature peak positions, widths (FWHM), and assignments.

Band	Position (eV)	Width (eV)	Vibrational modes <sup>a</sup>	Assignment
Elastic peak	0.00	0.08	$\nu_{19}, \nu_{26}, \nu_{27}$	Ring/CHO-twisting
Band I	0.12	0.11	$\nu_{5-18}$	CC-stretching/CH-
	0.22	0.11	$\nu_{20-25}$	Bending/CO-stretching
Band II	0.37	0.12	$\nu_{1-4}$	CH-stretch
Band III	0.55	0.13		Combination band
Band IV	0.70	0.13		2×CH-stretch

<sup>a</sup>IR and Raman vibrational frequencies have been assigned by Rogojev *et al.*, *Spectrochim. Acta, Part A* **61**, 1661 (2005).

in our measurements was  $\sim 80$  meV (FWHM), which was insufficient to resolve many of the vibrational modes from one another (see Table I). Consequently, composite vibrational mode cross sections are reported here (see Fig. 2). EELS were accumulated at each scattering angle and incident electron energy by recording the number of scattered electrons detected at each energy loss ( $E_L$ ) value. The true electron count rate at each  $E_L$  was recorded using a multichannel scaler (MCS) synchronised to a linear voltage ramp that varied the detected energy loss between  $-0.2$  and  $1.0$  eV (see Fig. 2). Using this approach, the EELS are built up by continually scanning over that range of  $E_L$  values, so that the effect of any variations in the target beam flux or incident electron current on a given EELS is minimised. EELS at each  $E_0$  and  $\theta$  were repeatedly measured (2–4 times) to ensure reproducibility of the inelastic to elastic peak ratios (see below) to within the experimental uncertainty.

The assignment of the furfural composite vibrational modes we observe (bands I–IV) follows that in the work of Rogojev *et al.*<sup>43</sup> and are summarised in Table I. The EELS were now deconvoluted into contributions arising from each individual or unresolved combination of excited vibrational states.<sup>44</sup> In each case, one or two Gaussian functions were used to describe the spectral profile for each resolvable inelastic feature and the elastic peak (see Table I), with a typical

example of the result from those fits (in which the peak energies and peak widths are fixed in each case) being given in Fig. 2. The amplitudes of the Gaussian functions were then varied in a least-squares fitting procedure<sup>44</sup> to provide the best fit to the measured spectra. The ratio ( $R$ ) of the area under the fitting function for each  $i$ th vibrational feature to that under the elastic peak, at each  $E_0$  and  $\theta$ , is quite simply related to the ratio of the differential cross sections (DCSs) ( $\sigma$ ) from

$$R_i(E_0, \theta) = \frac{\sigma_i(E_0, \theta)}{\sigma_0(E_0, \theta)}. \quad (1)$$

Note that Eq. (1) is only valid if the transmission efficiency of the analyser remains constant over the energy loss and angular range studied or is at least well characterised.<sup>42</sup> Following a technique similar to that of Allan,<sup>45</sup> an additional focussing lens (synchronised to the voltage ramp) was also used to minimise variations in the analyser transmission efficiency for electrons detected with different values of  $E_L$ . Of course in the present measurements, the scattered electron energies are all very similar to that for  $E_0$ , so that a significant transmission effect is not anticipated. Nonetheless, we place a conservative uncertainty of 20% on our efficiency being unity.<sup>46</sup> The present measured  $R_i$  for the composite vibrational mode bands I and II are summarised in Tables II and III, respectively. Values of  $R_i$  for bands III and IV are not reported as, despite the very long run times in acquiring the EELS, we do not believe they are of sufficient statistical quality in order to derive differential cross sections. This can be gleaned from Fig. 2. Perhaps this result is not too surprising as from infrared absorption spectra<sup>47</sup> we know that when the relevant potential surfaces are not particularly anharmonic, the intensity of the fundamental modes is significantly greater than either their combination or overtone modes. As band III is essentially a combination band while band IV is comprised of CH stretch overtones, the results embodied in Fig. 2 might in some sense have been anticipated. Nonetheless, we do use the bands III and IV data that we have collected to provide an upper bound estimate on their DCSs in the 20–40 eV impact energy range and over the angular range covered in our experiments.

TABLE II. Differential cross sections ( $\times 10^{-16}$  cm<sup>2</sup>/sr) for vibrational excitation of the composite CC and CO stretching and CH bending modes (Band I,  $E_L \sim 0.12$ – $0.22$  eV) of furfural.

Angle (deg)	$E_0 = 20$ eV			$E_0 = 30$ eV			$E_0 = 40$ eV		
	Ratio	DCS	Uncertainty (%)	Ratio	DCS	Uncertainty (%)	Ratio	DCS	Uncertainty (%)
10							$6.06 \times 10^{-3}$	$2.93 \times 10^{-1}$	71
15				$6.17 \times 10^{-3}$	$1.91 \times 10^{-1}$	69	$6.33 \times 10^{-3}$	$1.61 \times 10^{-1}$	68
20	$5.77 \times 10^{-3}$	$1.17 \times 10^{-1}$	73	$5.43 \times 10^{-3}$	$8.03 \times 10^{-2}$	64	$7.39 \times 10^{-3}$	$8.54 \times 10^{-2}$	61
25							$1.18 \times 10^{-2}$	$6.25 \times 10^{-2}$	69
30	$4.42 \times 10^{-2}$	$2.35 \times 10^{-1}$	65	$3.94 \times 10^{-2}$	$1.30 \times 10^{-1}$	25	$1.50 \times 10^{-2}$	$4.23 \times 10^{-2}$	32
40	$3.01 \times 10^{-2}$	$6.55 \times 10^{-2}$	51	$3.59 \times 10^{-2}$	$5.18 \times 10^{-2}$	26	$4.52 \times 10^{-2}$	$5.72 \times 10^{-2}$	27
50	$6.09 \times 10^{-2}$	$6.53 \times 10^{-2}$	70	$4.90 \times 10^{-2}$	$4.24 \times 10^{-2}$	23	$4.02 \times 10^{-2}$	$3.78 \times 10^{-2}$	23
60	$6.83 \times 10^{-2}$	$6.11 \times 10^{-2}$	23	$4.96 \times 10^{-2}$	$3.78 \times 10^{-2}$	23	$4.17 \times 10^{-2}$	$3.12 \times 10^{-2}$	24
70	$8.04 \times 10^{-2}$	$6.30 \times 10^{-2}$	23	$5.96 \times 10^{-2}$	$3.52 \times 10^{-2}$	22	$6.08 \times 10^{-2}$	$3.10 \times 10^{-2}$	22
80	$8.88 \times 10^{-2}$	$6.51 \times 10^{-2}$	23	$8.12 \times 10^{-2}$	$4.06 \times 10^{-2}$	44	$8.38 \times 10^{-2}$	$3.33 \times 10^{-2}$	23
90	$1.04 \times 10^{-1}$	$6.58 \times 10^{-2}$	25	$8.44 \times 10^{-2}$	$3.88 \times 10^{-2}$	22	$8.60 \times 10^{-2}$	$3.54 \times 10^{-2}$	23

TABLE III. Differential cross sections ( $\times 10^{-16}$  cm<sup>2</sup>/sr) for vibrational excitation of the composite CH stretching modes (Band II,  $E_L \sim 0.37$  eV) of furfural.

Angle (deg)	$E_0 = 20$ eV			$E_0 = 30$ eV			$E_0 = 40$ eV		
	Ratio	DCS	Uncertainty (%)	Ratio	DCS	Uncertainty (%)	Ratio	DCS	Uncertainty (%)
10							$4.34 \times 10^{-4}$	$2.10 \times 10^{-2}$	73
15				$4.39 \times 10^{-4}$	$1.36 \times 10^{-2}$	43	$3.42 \times 10^{-4}$	$8.71 \times 10^{-3}$	59
20	$9.19 \times 10^{-4}$	$1.86 \times 10^{-2}$	27	$7.11 \times 10^{-4}$	$1.05 \times 10^{-2}$	31	$6.57 \times 10^{-4}$	$7.59 \times 10^{-3}$	39
25							$1.26 \times 10^{-3}$	$6.67 \times 10^{-3}$	38
30	$7.28 \times 10^{-3}$	$3.87 \times 10^{-2}$	23	$3.40 \times 10^{-3}$	$1.12 \times 10^{-2}$	29	$1.91 \times 10^{-3}$	$5.37 \times 10^{-3}$	39
40	$4.73 \times 10^{-3}$	$1.03 \times 10^{-2}$	24	$2.79 \times 10^{-3}$	$4.02 \times 10^{-3}$	41	$5.21 \times 10^{-3}$	$6.60 \times 10^{-3}$	29
50	$7.76 \times 10^{-3}$	$8.32 \times 10^{-3}$	23	$3.85 \times 10^{-3}$	$3.33 \times 10^{-3}$	27	$3.93 \times 10^{-3}$	$3.70 \times 10^{-3}$	29
60	$1.03 \times 10^{-2}$	$9.21 \times 10^{-3}$	23	$3.81 \times 10^{-3}$	$2.91 \times 10^{-3}$	26	$4.49 \times 10^{-3}$	$3.36 \times 10^{-3}$	26
70	$1.21 \times 10^{-2}$	$9.50 \times 10^{-3}$	23	$4.66 \times 10^{-3}$	$2.75 \times 10^{-3}$	25	$4.98 \times 10^{-3}$	$2.54 \times 10^{-3}$	25
80	$1.24 \times 10^{-2}$	$9.09 \times 10^{-3}$	25	$5.46 \times 10^{-3}$	$2.73 \times 10^{-3}$	25	$6.37 \times 10^{-3}$	$2.54 \times 10^{-3}$	25
90	$1.20 \times 10^{-2}$	$7.56 \times 10^{-3}$	24	$6.20 \times 10^{-3}$	$2.85 \times 10^{-3}$	26	$5.71 \times 10^{-3}$	$2.35 \times 10^{-3}$	30

It is immediately apparent from Eq. (1) that the product  $R_i \times \sigma_0$  gives the required composite vibrational mode DCSs provided the elastic DCSs ( $\sigma_0$ ) are known. Those results, for bands I and II, can also be found in Tables II and III. In this study, we have utilised the parallel version of our Schwinger Multichannel with norm-conserving pseudopotentials (SMCPP) computation approach,<sup>48</sup> which incorporates single-excitation configuration interaction techniques for the target description, for the elastic DCSs at 20 eV, 30 eV, and 40 eV. Note that no measured elastic DCSs for electron scattering from furfural are currently published, and given the challenges we found in using furfural, we are sceptical that any applications of the relative flow technique<sup>49</sup> to attempt such measurements are likely. This follows as in using the relative flow method, one necessarily cycles the target and standard gases throughout the measurements.<sup>49</sup> In our experience, the furfural pressure took some time to stabilise, making the duty cycle in a relative flow measurement with it as the target species highly problematic. The efficacy of using our SMCPP approach, to effect the normalisation of our  $R_i$  via Eq. (1), is discussed in detail elsewhere.<sup>50</sup> Here we simply note that similar to what we found in our recent investigation in phenol,<sup>28</sup> we believe the elastic SMCPP results are a valid choice.

The current composite vibrational excitation DCSs for bands I and II in furfural are given in Tables II and III and plotted in Fig. 3. Error estimates in those data are also provided in each of these tables. Particular attention to the identification and quantification of all possible sources of error has been made in this investigation. Here the statistical errors associated with the scattering intensity measurements for the elastic peak and bands I and II are usually small ( $<2\%$ ). An additional error due to our analyser transmission calibration ( $\sim 20\%$ ) must also be considered. While the inherent error in our SMCPP elastic DCS computations is negligible, we have found from past experience<sup>28,48</sup> that it can often reproduce the experimental data to 10% or better between 20 and 40 eV. Hence, a 10% uncertainty on our elastic DCS has been incorporated into our analysis. Another important source of possible error is that associated with the numerical deconvolution of the energy loss spectra, so an allowance for that is also made in the overall inelastic DCS uncertainties.

When all these factors are combined in quadrature, the errors in our composite vibrational mode DCS (see Tables II and III) are usually found to be in the range 22%–73%. Note that the largest uncertainties typically occur at the more forward scattering angles, where the elastic scattering intensity is much larger than that for vibrational excitation. This can make it particularly challenging to uniquely resolve these features.

The DCS for a given scattering process,  $i$ , is related to the integral cross section (ICS),  $Q_i$ , through the standard formula

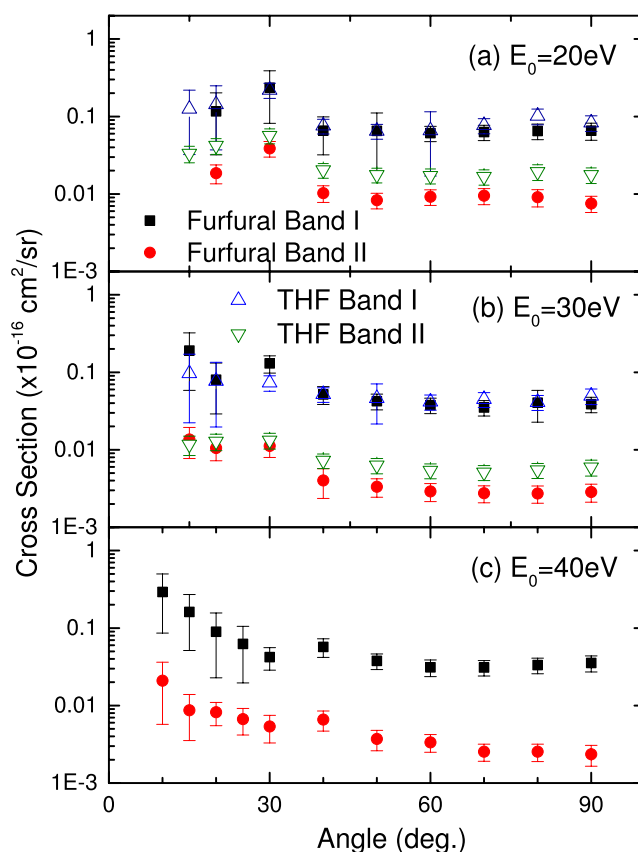


FIG. 3. Differential cross sections ( $\times 10^{-16}$  cm<sup>2</sup>/sr) for electron-impact excitation of the composite vibrational modes of furfural at impact energies of (a) 20 eV, (b) 30 eV, and (c) 40 eV. Also shown are DCS for electron impact excitation of THF.<sup>5</sup> See legend in figure for further details.

TABLE IV. Integral cross sections ( $\times 10^{-16}$  cm $^2$ ) for electron impact excitation of the experimentally assigned composite vibrational modes and their sum. The percentage uncertainties on these derived values are also presented. See text for more details.

$E_0$ (eV)	Band I ( $E_L \sim 0.12\text{--}0.22$ eV)		Band II ( $E_L \sim 0.37$ eV)		Sum of vibrationals	
	ICS	(%)	ICS	(%)	ICS	(%)
20	1.205	58	0.158	46	1.363	52
30	0.768	52	0.059	50	0.827	49
40	0.672	54	0.052	52	0.724	50

$$Q_i(E_0) = 2\pi \int_0^\pi \sigma_i(E_0, \theta) \sin \theta d\theta. \quad (2)$$

In order to convert experimental DCS data, measured at discrete angles that span a finite angular range determined by the physical constraints of the apparatus, to an ICS, one must first interpolate/extrapolate these DCS to cover the full angular range from  $0^\circ$  to  $180^\circ$ . Our approach to accomplish this has also been discussed in great detail previously<sup>25</sup> and so we do not repeat that detail again here. Rather, we simply note that the present ICSs, and the uncertainty on that data, are summarised in Table IV and plotted in Fig. 4. Note that the errors on our ICS, as well as incorporating those from the DCS (with allowance for the  $\sin \theta$  weighting factor in Eq. (2)), also include an uncertainty from the extrapolation of our DCS to  $0^\circ$  and  $180^\circ$ . When these factors are accounted for, the ICS errors are found to be in the range 46%–58%, with the precise error depending on the incident electron energy and composite vibrational mode in question.

### III. RESULTS AND DISCUSSION

In Tables II and III and Fig. 3, we present the differential cross section results, for electron impact excitation of the bands I and II composite vibrational modes in furfural, from

our experimental investigations. As noted in Table I, the dominant modes in band I relate to the CC-stretching, CH-bending, and CO-stretching modes, with the CO-stretching modes being predominant in terms of infrared intensity,<sup>43</sup> while the dominant modes in band II are assigned as being due to the CH-stretches. Furfural has two co-existing conformers, with the population of the *trans* conformer being  $\sim 79.5\%$  and that of the *cis* conformer being  $\sim 20.5\%$ . While Rogojev *et al.*<sup>43</sup> noted that the infrared frequency data of the respective normal modes of the two conformers are somewhat different, with our energy resolution such a small difference will not be observed. Also shown in Fig. 3 are corresponding bands I and II vibrational differential cross sections, at 20 eV and 30 eV, for electron impact excitation of THF from Do *et al.*<sup>5</sup> While, as noted previously (see Fig. 1), furfural and THF do have some structural similarities, their nuclear dynamics are in fact quite different. Specifically, THF has 33 normal modes of vibration while furfural has only 27 normal modes. However, in band I for furfural, 20 of those modes are encompassed while for THF, 22 modes are encompassed. Here these band I modes relate to CC-stretching and CH-bending in both furfural and THF. The comparable induced molecular vibrations and density of states may lead to similar DCS behaviour. On the other hand, in band II, furfural possesses only four CH-stretch modes while in THF there are eight. As a consequence, we might *a priori* anticipate that the band II DCSs in THF will be relatively stronger in magnitude than those for furfural. In addition, our derived integral cross section results are given in Table IV and plotted in Fig. 4. In this case, we compare the present ICSs to corresponding data in furan from Hargreaves *et al.*<sup>38</sup> Furan is also a structurally similar molecule to furfural (see Fig. 1), although it possesses only 21 normal modes of vibration compared, as noted above, to furfural's 27 modes. Therefore, purely on a density of states argument, we would expect the respective bands I and II ICSs for furfural to be larger than those for furan, although we are also interested in seeing if there is any discernible trend in the integral cross sections from both species. Note that in Table IV, we also

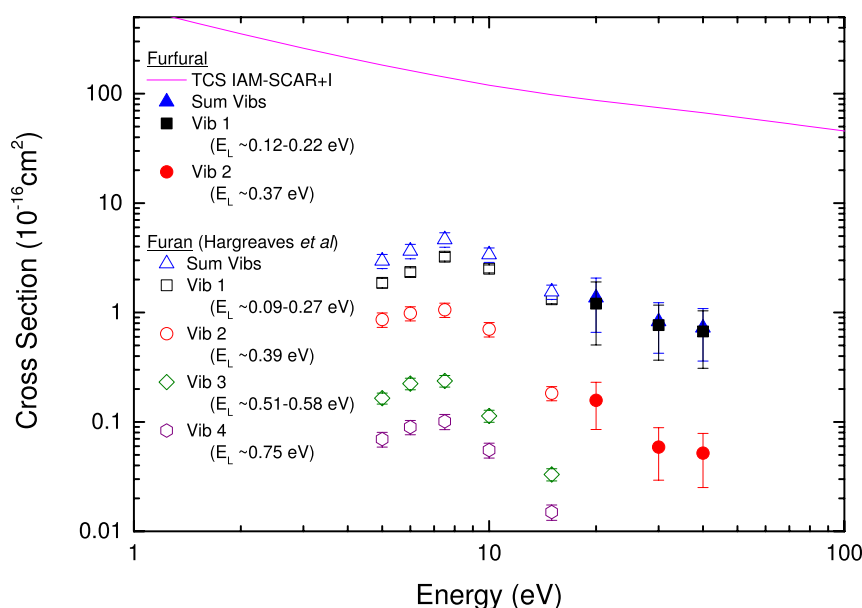


FIG. 4. Integral cross sections ( $\times 10^{-16}$  cm $^2$ ) for electron impact excitation of the composite vibrational bands of furfural and furan.<sup>38</sup> Also shown is the total cross section obtained at the IAM-SCAR+I level. See legend and text for details.

list the summed ICS values for bands I and II, with that data being plotted and compared to the furan ICS sum<sup>38</sup> in Fig. 4. All the errors listed in Tables II–IV and plotted in Figs. 3 and 4 are at the one standard deviation level.

Let us consider Fig. 3 in more detail. Here we observe that at each energy, the shapes of the furfural differential cross sections, i.e., their angular distributions, for bands I and II are very similar. In particular we find that at 20 eV, both angular distributions are quasi-isotropic, at 30 eV, there is just a suggestion for their DCS being more forward peaked at the smaller scattered electron angles, while at 40 eV, both angular distributions are now clearly forward peaked in magnitude at smaller  $\theta$ . The tendency for the angular distributions of composite vibrational modes to be quasi-isotropic, at energies  $\sim 15$ – $20$  eV, has been observed by us previously in THF,<sup>5</sup> THFA,<sup>7</sup> pyrimidine,<sup>8</sup> and phenol<sup>11</sup> and still awaits a definitive explanation from theory. The angular distribution results at 40 eV are more understandable in terms of the target molecular properties, in that they exhibit a behaviour consistent with furfural having both a strong permanent dipole moment ( $3.46$ – $3.57$  D<sup>51,52</sup> for the *trans* conformer), and a dipole polarisability of some magnitude ( $59.92$   $a_0^{3,53}$ ). In terms of the furfural band I and II DCS magnitudes, it is clear from Fig. 3 that the  $DCS_{\text{BandI}} \gg DCS_{\text{BandII}}$ , indeed often by an order of magnitude at each  $E_0$ . If we now compare the furfural and THF differential cross sections for band I, then to within the combined uncertainties on both sets of data and for each of 20 eV and 30 eV, we find them to be in remarkably good agreement (as was foreshadowed earlier). For band II, however, and again as anticipated earlier, we typically find the magnitude of the THF DCSs to be greater than those for the furfural DCSs. This is largely true at both energies where a comparison can be made, and in particular for  $\theta \geq 40^\circ$ . We reiterate that we believe this behaviour reflects that while band II in THF contains 8 normal modes in furfural it has only 4 normal modes that can be excited. In Fig. 2, it is also apparent that further bands of composite vibrational modes in furfural (bands III and IV) can be excited by electron impact. However, as noted previously, the statistical quality of that data was not considered to be high enough by us to report values for their cross sections. Nonetheless, the analysis carried out for bands I and II was repeated for bands III and IV so that we can estimate that the maximum (upper bound) DCSs for each of those bands, for  $E_0$  in the 20–40 eV range, will not exceed  $2 \times 10^{-19}$  cm<sup>2</sup>/sr (i.e., a very small cross section).

Consistent with what we found at the differential cross section level, we observe in Fig. 4 that the magnitude of the ICS for vibrational band I in furfural is significantly greater than for its band II, over the 20–40 eV energy range. In Fig. 4, we find that the trend in the energy dependence of the ICSs, for bands I and II in furan and furfural, appears to be in quite good accord, despite the fact there is no overlap in their measured energy range. If the ICS energy dependence seen in THF,<sup>6</sup> where the cross section decreases rapidly in magnitude in going from 10 to 20 eV, occurs in both furan and furfural, we would anticipate that the magnitude of the furfural ICS would be larger than for the corresponding bands in furan. This would be consistent with the aforementioned density of vibrational states for these species. This raises the interesting possibility

of appropriately scaled furan cross sections, in conjunction with the present furfural cross sections, being combined to assemble a reasonably complete vibrational excitation data base for furfural between 5 and 40 eV. Such a vibrational excitation cross section data base might ultimately be put to good use as a part of an extensive and benchmarked data set of cross sections, in modelling studies of the type described in Ness *et al.*,<sup>1</sup> de Urquijo *et al.*,<sup>2</sup> Duque *et al.*,<sup>6</sup> Muñoz *et al.*,<sup>15</sup> or Fuss *et al.*<sup>16</sup> One possible problem with this idea is whether or not the broad shape resonance, at  $E_0 \sim 7$ – $10$  eV, observed in the furan vibrational channels would also be found in furfural. We believe this is likely to be the case as structurally similar ring-based species such as THF,<sup>3,6,54</sup> THFA,<sup>7</sup> and even pyrimidine<sup>8</sup> all exhibit similar  $\pi^*$  shape resonances in that energy regime. In Fig. 4, we also plot total cross section (TCS) results from an IAM-SCAR computation, with interference (I) terms,<sup>55</sup> denoted as IAM-SCAR+I. Full details of this approach can be found in the work of da Costa *et al.*,<sup>50</sup> and so are not given in this paper. Rather, here we simply highlight that at the TCS level, and for  $E_0 \geq 20$  eV, there is a good body of evidence to suggest that the IAM-SCAR or IAM-SCAR+I calculations provide accurate TCS data.<sup>28,56,57</sup> As a consequence, the results embodied in Fig. 4, which suggest that the ICSs for the sum of the vibrational bands in furfural contribute only  $\sim 1\%$  of the TCS, between 20–40 eV, are likely to be correct. While this is clearly a very small contribution to the TCS, being dwarfed by the total ionisation cross section, for example,<sup>57</sup> it nonetheless cannot be ignored as shown for other systems in some of the modelling simulations we have cited.<sup>2,4,6</sup> Finally, Fig. 4 also demonstrates that the bands III and IV integral cross sections of furan<sup>38</sup> are much lower in magnitude than those found for bands I and II. That result is entirely consistent with what we have measured in furfural, as can be seen from the energy loss spectrum of Fig. 2.

#### IV. CONCLUSIONS

We have reported electron impact composite mode vibrational excitation cross sections in furfural, for incident electrons with energies in the 20–40 eV range. We believe those cross sections are original, with no other computational or experimental results on vibrational excitation in furfural currently being available in the literature. However, we hope the present investigation does stimulate further studies on this important “green” species. Nonetheless, by comparing the present cross sections to corresponding results from THF at the DCS level, and furan at the ICS level, we were able to glean a remarkable qualitative similarity between the angular distributions of furfural and THF, for both composite vibrational bands, and between the trend in the energy dependence of the ICSs, again for both composite bands, for furfural and furan. This similarity, over common energy regimes for vibrational excitation in structurally similar molecules, or at least between molecules with a common ring structural unit, is intriguing and we believe worthy of further consideration. The results from the present study, when combined with those from our other investigations into

furfural's electronic structure,<sup>36</sup> ionisation,<sup>37,58</sup> elastic and total scattering,<sup>50</sup> and discrete electronic-state excitation,<sup>58,59</sup> form the basis for assembling the sort of comprehensive data base ultimately needed to better understand the role of atmospheric-pressure low-temperature plasmas on biomass in order to produce biofuels, etc.

## ACKNOWLEDGMENTS

This work was supported by the Australian, Brazilian, and Spanish government funding agencies (ARC, CNPq, CAPES). D.B.J. thanks the ARC for a Discovery Early Career Researcher Award. R.F.C.N. acknowledges CNPq and Flinders University for financial assistance, while M.J.B. thanks CNPq for his "Special Visiting Professor" award. R.F.C., M.T.N.V., and M.A.P.L. acknowledge financial support from FAPESP, while R.F.C., M.T.N.V., M.H.F.B., M.C.A.L., and M.A.P.L. acknowledge financial support from CNPq. M.C.A.L. also acknowledges support from FAPEMIG. G.G. thanks the Spanish Ministerio de Economía y Competitividad under Project No. FIS2012-31230 and the European Union COST Action CM1301 for funding.

- <sup>1</sup>K. F. Ness, R. E. Robson, M. J. Brunger, and R. D. White, *J. Chem. Phys.* **136**, 024318 (2012).
- <sup>2</sup>J. de Urquijo, E. Basurto, A. M. Juárez, K. F. Ness, R. E. Robson, M. J. Brunger, and R. D. White, *J. Chem. Phys.* **141**, 014308 (2014).
- <sup>3</sup>N. A. Garland, M. J. Brunger, G. García, J. de Urquijo, and R. D. White, *Phys. Rev. A* **88**, 062712 (2013).
- <sup>4</sup>R. D. White, M. J. Brunger, N. A. Garland, R. E. Robson, K. F. Ness, G. García, J. de Urquijo, and Z. Lj. Petrović, *Eur. Phys. J. D* **68**, 125 (2014).
- <sup>5</sup>T. P. T. Do, H. V. Duque, M. C. A. Lopes, D. A. Konovalov, R. D. White, M. J. Brunger, and D. B. Jones, *J. Chem. Phys.* **142**, 124306 (2015).
- <sup>6</sup>H. V. Duque, T. P. T. Do, M. C. A. Lopes, D. A. Konovalov, R. D. White, M. J. Brunger, and D. B. Jones, *J. Chem. Phys.* **142**, 124307 (2015).
- <sup>7</sup>H. V. Duque, L. Chiari, D. B. Jones, Z. Pettifer, G. B. da Silva, P. Limão-Vieira, F. Blanco, G. García, R. D. White, M. C. A. Lopes, and M. J. Brunger, *J. Chem. Phys.* **140**, 214306 (2014).
- <sup>8</sup>D. B. Jones, L. Ellis-Gibblings, G. García, K. L. Nixon, M. C. A. Lopes, and M. J. Brunger, *J. Chem. Phys.* **143**, 094304 (2015).
- <sup>9</sup>E. M. de Oliveira, S. d'A Sanchez, M. H. F. Bettega, A. P. P. Natalense, M. A. P. Lima, and M. T. do N. Varella, *Phys. Rev. A* **86**, 020701(R) (2012).
- <sup>10</sup>E. M. de Oliveira, R. F. da Costa, S. d. A. Sanchez, A. P. P. Natalense, M. H. F. Bettega, M. A. P. Lima, and M. T. do N. Varella, *Phys. Chem. Chem. Phys.* **15**, 1682 (2013).
- <sup>11</sup>R. F. C. Neves, D. B. Jones, M. C. A. Lopes, K. L. Nixon, E. M. de Oliveira, R. F. da Costa, M. T. do N. Varella, M. H. F. Bettega, M. A. P. Lima, G. B. da Silva, and M. J. Brunger, *J. Chem. Phys.* **142**, 194302 (2015).
- <sup>12</sup>R. F. C. Neves, D. B. Jones, M. C. A. Lopes, F. Blanco, G. García, K. Ratnavelu, and M. J. Brunger, *J. Chem. Phys.* **142**, 194305 (2015).
- <sup>13</sup>A. G. Sanz, M. C. Fuss, A. Muñoz, F. Blanco, P. Limão-Vieira, M. J. Brunger, S. J. Buckman, and G. García, *Int. J. Radiat. Biol.* **88**, 71 (2012).
- <sup>14</sup>R. D. White, W. Tattersall, G. Boyle, R. E. Robson, S. Dujko, Z. Lj. Petrović, A. Bankovic, M. J. Brunger, J. P. Sullivan, S. J. Buckman, and G. García, *Appl. Radiat. Isotopes* **83**, 77 (2014).
- <sup>15</sup>A. Muñoz, F. Blanco, G. García, P. A. Thorn, M. J. Brunger, J. P. Sullivan, and S. J. Buckman, *Int. J. Mass Spectrom.* **277**, 175 (2008).
- <sup>16</sup>M. C. Fuss, L. Ellis-Gibblings, D. B. Jones, M. J. Brunger, F. Blanco, A. Muñoz, P. Limão-Vieira, and G. García, *J. Appl. Phys.* **117**, 214701 (2015).
- <sup>17</sup>R. E. Robson, M. J. Brunger, S. J. Buckman, G. García, Z. Lj. Petrović, and R. D. White, *Sci. Rep.* **5**, 12674 (2015).
- <sup>18</sup>J. Amorim, C. Oliveira, J. A. Souza-Corrêa, and M. A. Ridenti, *Plasma Processes Polym.* **10**, 670 (2013).
- <sup>19</sup>N. Schultz-Jensen, F. Leipold, H. Bindslev, and A. Thomsen, *Appl. Biochem. Biotechnol.* **163**, 558 (2011).
- <sup>20</sup>P. A. Thorn, M. J. Brunger, P. J. O. Teubner, N. Diakomichalis, T. Maddern, M. A. Bolorizadeh, W. R. Newell, H. Kato, M. Hoshino, H. Tanaka, H. Cho, and Y.-K. Kim, *J. Chem. Phys.* **126**, 064306 (2007).
- <sup>21</sup>M. J. Brunger, P. A. Thorn, L. Campbell, N. Diakomichalis, H. Kato, H. Kawahara, M. Hoshino, H. Tanaka, and Y.-K. Kim, *Int. J. Mass Spectrom.* **271**, 80 (2008).
- <sup>22</sup>T. P. T. Do, M. Leung, M. Fuss, G. García, F. Blanco, K. Ratnavelu, and M. J. Brunger, *J. Chem. Phys.* **134**, 144302 (2011).
- <sup>23</sup>H. V. Duque, L. Chiari, D. B. Jones, P. A. Thorn, Z. Pettifer, G. B. da Silva, P. Limão-Vieira, D. Duflot, M.-J. Hubin-Franskin, J. Delwiche, F. Blanco, G. García, M. C. A. Lopes, K. Ratnavelu, R. D. White, and M. J. Brunger, *Chem. Phys. Lett.* **608**, 161 (2014).
- <sup>24</sup>L. Chiari, H. V. Duque, D. B. Jones, P. A. Thorn, Z. Pettifer, G. B. da Silva, P. Limão-Vieira, D. Duflot, M.-J. Hubin-Franskin, J. Delwiche, F. Blanco, G. García, M. C. A. Lopes, K. Ratnavelu, R. D. White, and M. J. Brunger, *J. Chem. Phys.* **141**, 024301 (2014).
- <sup>25</sup>Z. Mašín, J. D. Gorfinkiel, D. B. Jones, S. M. Bellm, and M. J. Brunger, *J. Chem. Phys.* **136**, 144310 (2012).
- <sup>26</sup>D. B. Jones, S. M. Bellm, P. Limão-Vieira, and M. J. Brunger, *Chem. Phys. Lett.* **535**, 30 (2012).
- <sup>27</sup>D. B. Jones, S. M. Bellm, F. Blanco, M. Fuss, G. García, P. Limão-Vieira, and M. J. Brunger, *J. Chem. Phys.* **137**, 074304 (2012).
- <sup>28</sup>R. F. da Costa, E. M. de Oliveira, M. H. F. Bettega, M. T. do N. Varella, D. B. Jones, M. J. Brunger, F. Blanco, R. Colmenares, P. Limão-Vieira, G. García, and M. A. P. Lima, *J. Chem. Phys.* **142**, 104304 (2015).
- <sup>29</sup>R. F. C. Neves, D. B. Jones, M. C. A. Lopes, K. L. Nixon, G. B. da Silva, H. V. Duque, E. M. de Oliveira, R. F. da Costa, M. T. do N. Varella, M. H. F. Bettega, M. A. P. Lima, K. Ratnavelu, G. García, and M. J. Brunger, *J. Chem. Phys.* **142**, 104305 (2015).
- <sup>30</sup>A. S. Mammen, J.-M. Lee, Y.-C. Kim, I. T. Hwang, N.-J. Park, Y. K. Hwang, J.-S. Chang, and J.-S. Hwang, *Biofuels, Bioprod. Biorefin.* **2**, 438 (2008).
- <sup>31</sup>H. Gomez Bernal, L. Bornazzami, and A. M. Raspolli Galletti, *Green Chem.* **16**, 3734 (2014).
- <sup>32</sup>J.-P. Lange, E. van der Heide, J. van Buijtenen, and R. Price, *ChemSusChem* **5**, 150 (2012).
- <sup>33</sup>A. J. Ragauskas, C. K. Williams, B. H. Davison, G. Britovsek, J. Cairney, C. A. Eckert, W. J. Frederick, J. P. Hallett, D. J. Leak, C. L. Liotta, J. R. Mielenz, R. Murphy, R. Templer, and T. Tschaplinski, *Science* **311**, 484 (2006).
- <sup>34</sup>J. S. Bak, J. K. Ko, Y. H. Han, B. C. Lee, I.-G. Choi, and K. H. Kim, *Bioresour. Technol.* **100**, 1285 (2009).
- <sup>35</sup>A. W. Khan, J. P. Labrie, and J. McKeown, *Biotechnol. Bioeng.* **28**, 1449 (1986).
- <sup>36</sup>F. Ferreira da Silva, E. Lange, P. Limão-Vieira, N. C. Jones, S. V. Hoffmann, M.-J. Hubin-Franskin, J. Delwiche, M. J. Brunger, R. F. C. Neves, M. C. A. Lopes, E. M. de Oliveira, R. F. da Costa, M. T. do N. Varella, M. H. F. Bettega, F. Blanco, G. García, M. A. P. Lima, and D. B. Jones, *J. Chem. Phys.* **143**, 144308 (2015).
- <sup>37</sup>D. B. Jones, E. Ali, K. L. Nixon, P. Limão-Vieira, M.-J. Hubin-Franskin, J. Delwiche, C. G. Ning, J. Colgan, A. J. Murray, D. H. Madison, and M. J. Brunger, *J. Chem. Phys.* **143**, 184310 (2015).
- <sup>38</sup>L. R. Hargreaves, R. Albaridy, G. Serna, M. C. A. Lopes, and M. A. Khakoo, *Phys. Rev. A* **84**, 062705 (2011).
- <sup>39</sup>O. Zatsarinny, K. Bartschat, G. García, F. Blanco, L. R. Hargreaves, D. B. Jones, R. Murrin, J. R. Brunton, M. J. Brunger, M. Hoshino, and S. J. Buckman, *Phys. Rev. A* **83**, 042702 (2011).
- <sup>40</sup>H. Kato, A. Suga, M. Hoshino, F. Blanco, G. García, P. Limão-Vieira, M. J. Brunger, and H. Tanaka, *J. Chem. Phys.* **136**, 134313 (2012).
- <sup>41</sup>M. Fuss, A. G. Sanz, F. Blanco, P. Limão-Vieira, M. J. Brunger, and G. García, *Eur. Phys. J. D* **68**, 161 (2014).
- <sup>42</sup>M. J. Brunger and P. J. O. Teubner, *Phys. Rev. A* **41**, 1413 (1990).
- <sup>43</sup>M. Rogojevov, G. Keresztury, and B. Jordanov, *Spectrochim. Acta, Part A* **61**, 1661 (2005).
- <sup>44</sup>L. Campbell, M. J. Brunger, P. J. O. Teubner, B. Mojarrabi, and D. C. Cartwright, *Aust. J. Phys.* **50**, 525 (1997).
- <sup>45</sup>M. Allan, *J. Phys. B* **38**, 3655 (2005).
- <sup>46</sup>H. Tanaka, M. J. Brunger, L. Campbell, H. Kato, M. Hoshino, and A. R. P. Rau, "Utilizing scaled plane-wave Born cross sections for atoms and molecules," *Rev. Mod. Phys.* (submitted).
- <sup>47</sup>See <http://cccbdb.nist.gov/> for an IR spectrum.
- <sup>48</sup>R. F. da Costa, M. T. do N. Varella, M. H. F. Bettega, and M. A. P. Lima, *Eur. Phys. J. D* **69**, 159 (2015).
- <sup>49</sup>M. J. Brunger and S. J. Buckman, *Phys. Rep.* **357**, 215 (2002).
- <sup>50</sup>R. F. da Costa, M. T. do N. Varella, M. H. F. Bettega, F. Blanco, G. García, D. B. Jones, M. J. Brunger, and M. A. P. Lima, "Elastic electron collisions with furfural: An investigation on the behaviour of the cross sections under the influence of multichannel coupling effects" (unpublished).



- <sup>51</sup>D. R. Lide, *CRC Handbook of Chemistry and Physics*, 90th ed. (CRC Press, Boca Raton, FL, 2010).
- <sup>52</sup>R. Rivelino, S. Canuto, and K. Coutinho, *Braz. J. Phys.* **34**, 84 (2004).
- <sup>53</sup>T. Jewison, C. Knox, V. Neveu, Y. Djoumbou, A. C. Guo, J. Lee, P. Liu, R. Mandal, R. Krishnamurthy, I. Sinelnikov, M. Wilson, and D. S. Wishart, *Nucleic Acids Res.* **40**, D815 (2012).
- <sup>54</sup>A. Zecca, C. Perazzolli, and M. J. Brunger, *J. Phys. B* **38**, 2079 (2005).
- <sup>55</sup>F. Blanco and G. García, *Chem. Phys. Lett.* **635**, 321 (2005).
- <sup>56</sup>M. C. Fuss, A. G. Sanz, F. Blanco, J. C. Oller, P. Limão-Vieira, M. J. Brunger, and G. García, *Phys. Rev. A* **88**, 042702 (2013).
- <sup>57</sup>A. G. Sanz, M. C. Fuss, F. Blanco, J. D. Gorfinkiel, D. Almeida, F. Ferreira da Silva, P. Limão-Vieira, M. J. Brunger, and G. García, *J. Chem. Phys.* **139**, 184310 (2013).
- <sup>58</sup>D. B. Jones, R. F. da Costa, M. T. do N. Varella, M. H. F. Bettega, M. A. P. Lima, F. Blanco, G. García, and M. J. Brunger, "Integral elastic, electronic-state, ionization and total cross sections for electron scattering with furfural" (unpublished).
- <sup>59</sup>D. B. Jones, R. F. C. Neves, M. C. A. Lopes, R. F. da Costa, M. T. do N. Varella, M. H. F. Bettega, M. A. P. Lima, F. Blanco, G. García, P. Limão-Vieira, and M. J. Brunger, "Theoretical and experimental differential cross sections for electron impact excitation of the electronic bands of furfural" (unpublished).